

# Continuous Countercurrent Flow Model for a Bulk PSA Separation Process

S. Farooq  
D.M. Ruthven

Department of Chemical Engineering  
University of New Brunswick  
Fredericton, NB Canada E3B 5A3

The steps involved in a basic Skarstrom pressure swing adsorption (PSA) cycle are pressurization, high-pressure adsorption, countercurrent blowdown, and countercurrent purge, as represented in Figure 1a. If mass transfer between solid and gas phases during the pressurization and the blowdown steps is assumed to be negligible, then at cyclic steady state the amount adsorbed during the adsorption step should be equal to the amount desorbed during the purge step. Transient PSA simulation with a frozen solid approximation during pressurization and blowdown has been validated for processes of purification (Chihara and Suzuki, 1983a,b; Raghavan et al., 1985; Hassan et al., 1985) and kinetically controlled bulk separation (Hassan et al., 1986, 1987). Therefore, for these processes, Skarstrom PSA operation at cyclic steady state can be viewed as a continuous countercurrent flow (CCF) system in which the immobile solid phase adsorbs from the high-pressure stream and releases to the low-pressure purge stream with zero net accumulation in the solid phase, Figure 1b.

Suzuki (1985) developed a CCF model for a trace component PSA system and showed that the resultant steady-state concentration profiles match with those from the transient simulation using a frozen solid approximation during pressurization and blowdown and a small throughput ratio so that solid- and gas-phase profiles also remain nearly frozen during the adsorption and the desorption steps. While these extreme assumptions may be realistic for a purification process, in a bulk separation process there generally will be significant excursions of the concentration profiles during the adsorption and the desorption steps. The purpose of this communication is to examine the usefulness of the CCF model for a bulk PSA separation process.

## Theoretical Model

We consider an isothermal, plug flow system in which frictional pressure drop in the bed is negligible and the total pressure in the bed remains constant during the adsorption and the desorption steps. The equations are developed for a two-compo-

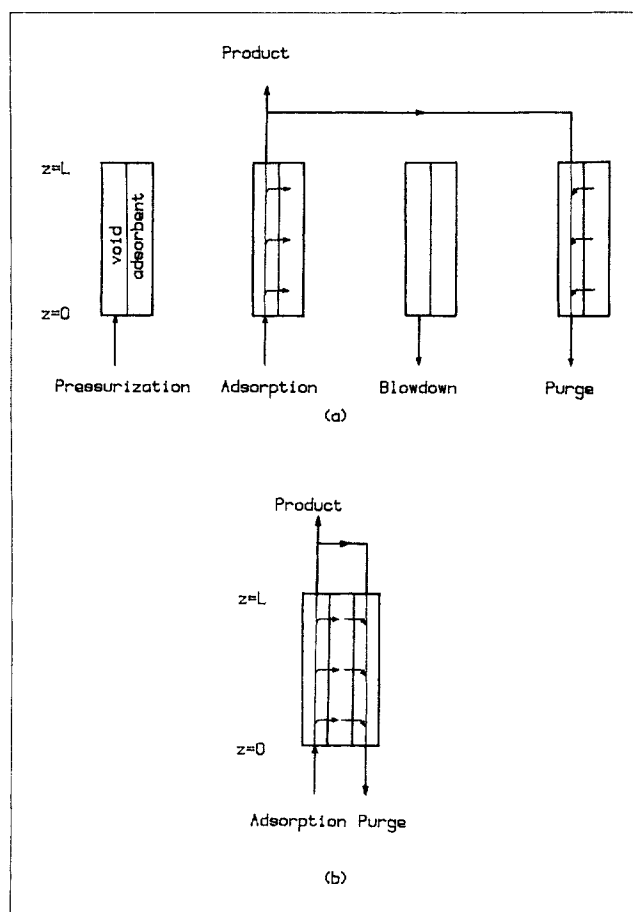


Figure 1. (a) Skarstrom PSA cycle.  
(b) Continuous countercurrent flow representation of a Skarstrom PSA cycle.

**Table 1. Kinetic and Equilibrium Data and Other Common Parameter Values Used in Simulations**

Feed composition	21% oxygen, 79% nitrogen
Adsorbent	CMS (Bergbau Forschung)
Bed length, cm	35
Bed radius, cm	1.75
Particle size, cm	0.3175 (pellet)
Particle density, g/cm <sup>3</sup>	0.9877
Bed voidage	0.40
Temperature, °C	25 (ambient)
Adsorption pressure, atm	3.0
Purge pressure, atm	1.0
Equilibrium constant for oxygen, $K_A$	9.25
Equilibrium constant for nitrogen, $K_B$	8.9
Saturation constant for oxygen, $q_{AS}$ , gmol/cm <sup>3</sup>	$2.64 \times 10^{-3}$
Saturation constant for nitrogen, $q_{BS}$ , gmol/cm <sup>3</sup>	$2.64 \times 10^{-3}$
Diffusional time constant for oxygen, $D/r^2$ , s <sup>-1</sup>	$3.73 \times 10^{-3}$
Diffusional time constant for nitrogen, $D/r^2$ , s <sup>-1</sup>	$1.17 \times 10^{-4}$

Values taken from Hassan et al. (1986)

nent system in which both the components are adsorbed and therefore the fluid velocity in the bed varies along the length of the column. Equilibrium relationships for both components are represented by the binary Langmuir isotherm and the mass transfer rates are given by linear driving force rate expressions. Development of the CCF model, subject to these assumptions, is as follows:

Mass balance (component  $A$ )

$$j \frac{d(u_i c_{Ai})}{dz} + \frac{1-\epsilon}{\epsilon} (m-1+j\alpha) \frac{dq_{Ai}}{dt} = 0 \quad (1)$$

Continuity condition

$$c_{Ai} + c_{Bi} = C_i \quad (\text{constant}) \quad (2)$$

Overall balance

$$jC_i \frac{du_i}{dz} + \frac{1-\epsilon}{\epsilon} (m-1+j\alpha) \left( \frac{dq_{Ai}}{dt} + \frac{dq_{Bi}}{dt} \right) = 0 \quad (3)$$

Mass transfer rates

$$\frac{dq_{Ai}}{dt} = k_{Ai} (q_{Ai}^* - q_{Ai}) \quad (4)$$

$$\frac{dq_{Bi}}{dt} = k_{Bi} (q_{Bi}^* - q_{Bi}) \quad (5)$$

Adsorption equilibrium

$$\frac{q_{Ai}^*}{q_{AS}} = \frac{b_A c_{Ai}}{1 + b_A c_{Ai} + b_B c_{Bi}} \quad (6)$$

$$\frac{q_{Bi}^*}{q_{BS}} = \frac{b_B c_{Bi}}{1 + b_A c_{Ai} + b_B c_{Bi}} \quad (7)$$

In the above equations  $i = H$  or  $L$ ,  $j = +1$  or  $-1$ , and  $m = 1$  or  $2$ . The values  $i = H$ ,  $j = +1$ , and  $m = 1$  represent high-pressure flow;  $i = L$ ,  $j = -1$ , and  $m = 2$  represent purge flow.

Boundary conditions for the high-pressure flow are:

$$c_{AH|z=0} = c_{AO} \quad (8)$$

$$u_{H|z=0} = u_{OH} \quad (9)$$

Boundary conditions for the purge flow are:

$$c_{AL|z=L} = c_{AH|z=L} \left( \frac{P_L}{P_H} \right) \quad (10)$$

$$u_{L|z=L} = u_{OL} \quad (11)$$

The velocities used in the above equations are the equivalent velocities for the CCF model and are related to the velocities in an actual PSA cycle as follows:

$$u_H = \alpha v_H; \quad u_{OH} = \alpha v_{OH} \quad (12)$$

$$u_L = (1 - \alpha) v_L; \quad u_{OL} = (1 - \alpha) v_{OL} \quad (13)$$

$$\alpha = \frac{t_H}{t_H + t_L} \quad (14)$$

Equation 10 represents the fact that part of the high-pressure product is expanded to low pressure and used for purge flow. In

**Table 2. Summary of Experimental Conditions, Product Purity, and Recovery\***

Exp. No.	$G$	$L/v$	Duration of Adsorption/Desorption Steps	Oxygen in Product, %			Recovery of Nitrogen, %	
				Exp	Trans. Model	CCF Model	Trans. Model	CCF Model
3	1.65	25	60	1.5	1.48	0.35	8.0	15.98
6	1.0	20	60	4.2	4.49	2.48	31.6	47.25
7	1.0	25	60	2.95	2.70	1.27	24.5	43.67
8	1.0	30	60	2.45	2.01	0.57	26.24	40.31
11	0.5	25	60	6.8	4.86	5.55	45.3	65.27

\* $k = \Omega (D/r^2)$ . Continuous counter current flow (CCF) model results computed with  $\Omega = 15$  for both oxygen and nitrogen. Experimental conditions and results and transient model predictions taken from Hassan (1985) and Hassan et al. (1986).

an actual operation,

$$v_{OL} = G \cdot v_{OH} \quad (15)$$

where  $G$  is the purge to feed velocity ratio. The equivalent relation for the CCF model will be:

$$u_{OL} = G \left( \frac{1 - \alpha}{\alpha} \right) u_{OH} \quad (16)$$

The factor  $(m - 1 + j\alpha)$  in Eqs. 1 and 3 has been introduced to maintain consistency in mass transfer rates between the CCF approximation and the transient simulation. The assumption of zero net accumulation in the solid phase leads to:

$$\alpha \frac{dq_{AH}}{dt} + (1 - \alpha) \frac{dq_{AL}}{dt} = 0 \quad (17)$$

$$\alpha \frac{dq_{BH}}{dt} + (1 - \alpha) \frac{dq_{BL}}{dt} = 0 \quad (18)$$

From Eqs. 4 and 17 we get:

$$q_A = \frac{\alpha k_{AH} q_{AH}^* + (1 - \alpha) k_{AL} q_{AL}^*}{\alpha k_{AH} + (1 - \alpha) k_{AL}} \quad (19)$$

Similarly, from Eqs. 5 and 18 we get:

$$q_B = \frac{\alpha k_{BH} q_{BH}^* + (1 - \alpha) k_{BL} q_{BL}^*}{\alpha k_{BH} + (1 - \alpha) k_{BL}} \quad (20)$$

Substituting Eq. 19 in Eq. 4 and Eq. 20 in Eq. 5 and rearranging yields:

$$(m - 1 + j\alpha) \frac{dq_{Ai}}{dt} = jk_{eA} (q_{AH}^* - q_{AL}^*) \quad (21)$$

$$(m - 1 + j\alpha) \frac{dq_{Bi}}{dt} = jk_{eB} (q_{BH}^* - q_{BL}^*) \quad (22)$$

where

$$k_{eA} = \frac{1}{\frac{1}{\alpha k_{AH}} + \frac{1}{(1 - \alpha) k_{AL}}} \quad (23)$$

$$k_{eB} = \frac{1}{\frac{1}{\alpha k_{BH}} + \frac{1}{(1 - \alpha) k_{BL}}} \quad (24)$$

Combining Eqs. 1, 3, 21, and 22 gives:

$$u_i \frac{dc_{Ai}}{dz} + \frac{1 - \epsilon}{\epsilon} [(1 - X_{Ai}) k_{eA} (q_{AH}^* - q_{AL}^*) - X_{Ai} k_{eB} (q_{BH}^* - q_{BL}^*)] = 0 \quad (25)$$

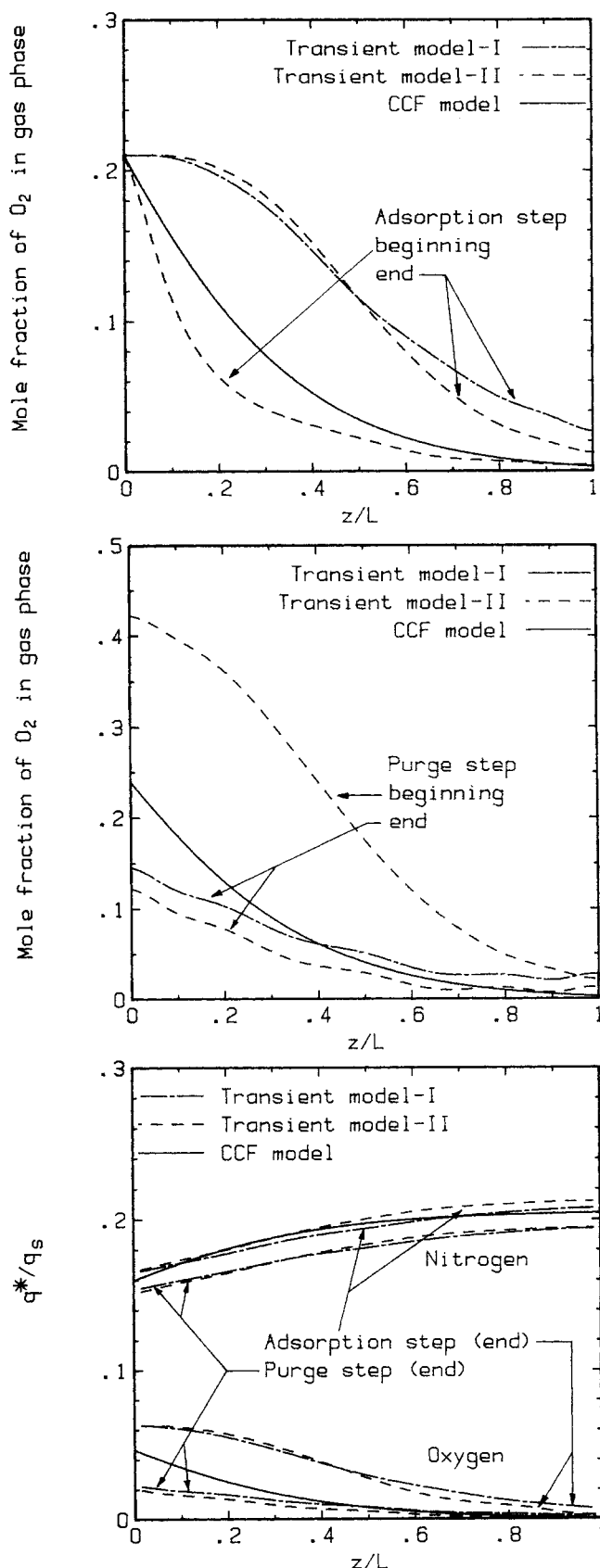


**Figure 2. Steady state concentration profiles from transient model and continuous countercurrent flow model.**

$G = 1.65$ ,  $L/v = 25$ , ads/des time = 90 s  
Other parameters as in Table 1.

Combining Eqs. 3, 21, and 22 results in:

$$C_i \frac{du_i}{dz} + \frac{1-\epsilon}{\epsilon} [k_{eA}(q_{AH}^* - q_{AL}^*) + k_{eB}(q_{BH}^* - q_{BL}^*)] = 0 \quad (26)$$

Equations 25 and 26 were integrated using the fourth-order Runge-Kutta method to obtain  $c_{Ai}$  and  $u_i$  at different axial locations in the bed. The boundary conditions at high-pressure flow are known at  $z = 0$  and those for purge are given at  $z = L$ , therefore the solution procedure required iteration. Values of the dependent variables for purge flow were guessed at  $z = 0$ . The integration was then performed from  $z = 0$  to  $z = L$ , which was repeated until the known boundary conditions for purge flow at  $z = L$  were satisfied. Jacobian analysis was performed to update the trial values. Starting from the same initial guess, the convergence was much faster with Jacobian analysis than without, as expected. Values  $c_{Bi}$  at different locations were obtained by difference from total concentration. Steady state adsorbed phase concentrations were then calculated from Eqs. 19 and 20.

## Results and Discussion

In order to assess the usefulness of the CCF model for a bulk PSA separation process, air separation on carbon molecular sieve, studied by Hassan et al. (1986), was selected. The kinetic and equilibrium data and other common parameters used in this study are given in Table 1. Purity and recovery predictions of the CCF model have been compared with the transient model pre-

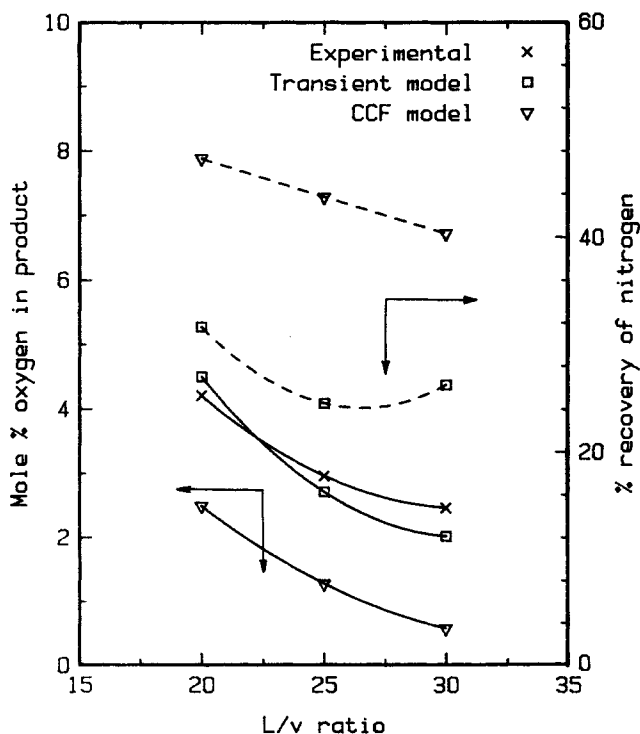


**Figure 3. Effect of  $L/v$  ratios on product purity and recovery.**  
Experimental conditions correspond to exp. nos. 6–8 in Table 2  
Other parameters as in Table 1

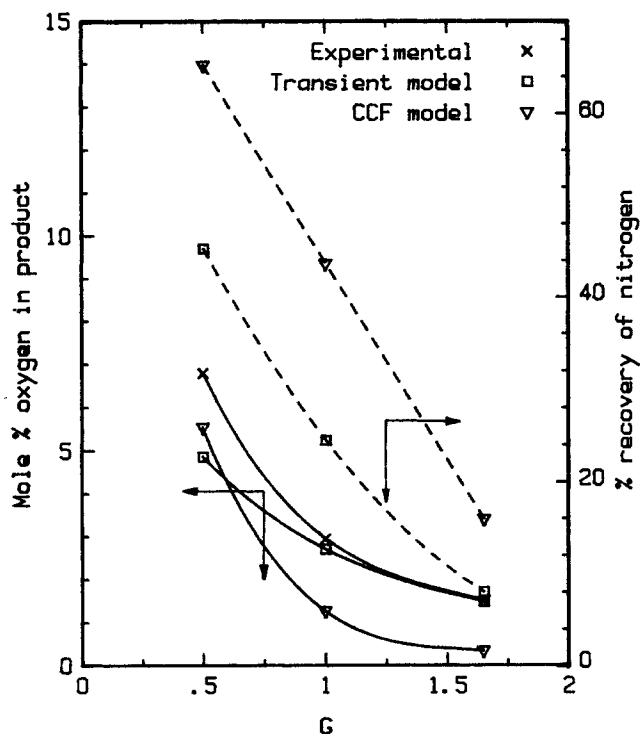


**Figure 4. Effect of purge to feed velocity ratio on product purity and recovery.**

Common parameters given in Table 1; for experimental conditions see exp. nos. 3, 7, 11 in Table 2.

dictions as well as the experimental results for a number of different operating conditions, summarized in Table 2.

Gas- and solid-phase concentration profiles in the bed predicted by the transient model at cyclic steady state are compared with the profiles given by the CCF model in Figure 2. The transient model profiles are shown for two extreme conditions. The frozen solid approximation during pressurization and blowdown has been taken as one extreme (transient model I). In the other extreme (transient model II) we assume that the pressure changes instantaneously during pressurization and blowdown and then mass transfer takes place between solid and gas phases under constant high and low pressures, respectively. It is interesting to note that the solid phase concentration profiles from the CCF model broadly represent the mean of concentration excursions during the adsorption and the desorption steps as predicted by the transient simulations irrespective of the assumptions made for pressurization and blowdown. Therefore, mass transfer during the pressurization and the blowdown steps will not impair the predictions of the CCF model.

The effects of  $L/v$  ratio and purge to feed velocity ratio on the purity and recovery of the nitrogen product are shown in Figures 3 and 4, respectively. The CCF model predicts the correct qualitative trend as observed experimentally, although the transient model is quantitatively superior.

The computations were carried out using an IBM 3090 (model 180) computer. Transient simulation, starting from clean bed initial conditions, required 30 to 40 CPU sec to reach cyclic steady state, dependent on parameter values. The iterative solutions of the CCF model, depending on the initial guess, required only 0.3 to 3.5 CPU sec.

The simulations, with other operating conditions similar to those in the caption of Figure 2, were repeated for diffusivities reduced by a factor of 10 and it was observed that the excursions of the concentration profiles were greatly reduced, thus reducing the quantitative differences between the transient model and the CCF model predictions. The agreement between the two models, shown by Suzuki (1985) for rapid cycling (i.e., extremely small throughput ratio) for air dehumidification, should also hold for a bulk separation process under similar conditions. However, even short of these extreme limits of very low diffusivities or very small throughput ratios, the CCF model still correctly predicts the qualitative trends of purity and recovery.

The present model solution is invariant to changes in cycle time as long as the durations of the adsorption and the desorption steps are kept equal. Other than that, the simplicity and computational efficiency of the model should be useful at least for selecting the range of conditions within which more detailed studies should be concentrated.

## Notation

- $b$  = Langmuir constant,  $\text{cm}^3/\text{gmol}$
- $c$  = gas phase concentration,  $\text{gmol}/\text{cm}^3$
- $C$  = total gas phase concentration,  $\text{gmol}/\text{cm}^3$
- $D$  = micropore diffusivity,  $\text{cm}^2/\text{s}$
- $G$  = purge to feed velocity ratio
- $k$  = LDF rate coefficient,  $\text{s}^{-1}$
- $K$  = adsorption equilibrium constant
- $L$  = bed length,  $\text{cm}$
- $P$  = column pressure,  $\text{atm}$
- $q$  = adsorbed phase concentration,  $\text{gmol}/\text{cm}^3$
- $q^*$  = adsorbed phase concentration in equilibrium with  $c$ ,  $\text{gmol}/\text{cm}^3$
- $r$  = crystal radius,  $\text{cm}$
- $t$  = time,  $\text{s}$
- $u$  = equivalent interstitial velocity for CCF model,  $\text{cm}/\text{s}$
- $v$  = interstitial velocity in an actual PSA operation,  $\text{cm}/\text{s}$
- $X$  = mole fraction in gas phase
- $z$  = axial distance,  $\text{cm}$

## Greek letters

- $\epsilon$  = bed voidage
- $\alpha$  = defined by Eq. 14
- $\Omega$  = constant in LDF rate expression

## Subscripts

$AO$  = component  $A$  in feed

$AH, AL, AS$  = component  $A$  at high pressure, purge pressure, saturation

$BH, BL, BS$  = component  $B$  at high pressure, purge pressure, saturation

$eA$  = equivalent for CCF model for component  $A$

$eB$  = equivalent for CCF model for component  $B$

$H$  = high-pressure flow

$L$  = purge flow

$OH$  = at the inlet of high-pressure flow

$OL$  = at the inlet of purge flow

## Literature Cited

- Chihara, K., and M. Suzuki, "Simulation of Nonisothermal Pressure Swing Adsorption," *J. Chem. Eng. Japan*, **16**, 53 (1983a).
- , "Air Drying by Pressure Swing Adsorption," *J. Chem. Eng. Japan*, **16**, 293 (1983b).
- Hassan, M. M., "Theoretical and Experimental Studies of Pressure Swing Adsorption-Systems," Ph.D. Diss., Univ. New Brunswick, Canada (1985).
- Hassan, M. M., N. S. Raghavan, D. M. Ruthven, and H. A. Boniface, "Pressure Swing Adsorption. II," *AIChE J.*, **31**, 2008 (1985).
- Hassan, M. M., N. S. Raghavan, and D. M. Ruthven, "Air Separation by Pressure Swing Adsorption on a Carbon Molecular Sieve," *Chem. Eng. Sci.*, **41**, 1333 (1986).
- , "Pressure Swing Adsorption Air Separation on a Carbon Molecular Sieve. II," *Chem. Eng. Sci.*, **42**, 2037 (1987).
- Raghavan, N. S., M. M. Hassan, and D. M. Ruthven, "Numerical Simulation of a PSA System. I," *AIChE J.*, **31**, 385 (1985).
- Suzuki, M., "Continuous Countercurrent Flow Approximation for Dynamic Steady State Profiles of Pressure Swing Adsorption," *AIChE Symp. Ser.* **81**(242), 67 (1985).

Manuscript received Aug. 16, 1989.